Electroweak physics in the forward region

Lake Louise Winter Institute

Marek Sirendi
on behalf of the LHCb Collaboration

University of Cambridge

February 16, 2015

New results from LHCb

Measurement of the forward W boson cross-section in pp collisions at $\sqrt{s} = 7\,\mathrm{TeV}$

JHEP12 (2014) 079 arXiv:1408.4354

Abstract

A measurement of the inclusive $W \to \mu\nu$ production cross-section using data from pp collisions at a centre-of-mass energy of $\sqrt{s} = 7\,\mathrm{TeV}$ is presented. The analysis is based on an integrated luminosity of about $1.0\,\mathrm{fb}^{-1}$ recorded with the LHCb detector. Results are reported for muons with a transverse momentum greater than $20\,\mathrm{GeV}/c$ and pseudorapidity between 2.0 and 4.5. The W^+ and W^- production cross-sections are measured to be

$$\sigma_{W^+\to\mu^+\nu} = 861.0 \pm 2.0 \pm 11.2 \pm 14.7\,\mathrm{pb},$$
$$\sigma_{W^-\to\mu^-\bar{\nu}} = 675.8 \pm 1.9 \pm 8.8 \pm 11.6\,\mathrm{pb},$$

where the first uncertainty is statistical, the second is systematic and the third is due to the luminosity determination. Cross-section ratios and differential distributions as functions of the muon pseudorapidity are also presented. The ratio of W^+ to W^- cross-sections in the same fiducial kinematic region is determined to be

$$\frac{\sigma_{W^+\to\mu^+\nu}}{\sigma_{W^-\to\mu^-\bar{\nu}}} = 1.274 \pm 0.005 \pm 0.009,$$

where the uncertainties are statistical and systematic, respectively. Results are in good agreement with theoretical predictions at next-to-next-to-leading order in perturbative quantum chromodynamics.

Measurement of forward $Z \to e^+e^-$ production at $\sqrt{s} = 8\,\mathrm{TeV}$

LHCb-PAPER-2015-003

Abstract

A measurement of the cross-section for Z-boson production in the forward region at 8 TeV centre-of-mass energy is presented. The measurement is based on a sample of $Z \to e^+e^-$ decays reconstructed using the LHCb detector corresponding to an integrated ... surement is defined ... apidities and trans... mass is required t... o be

Preliminary

σ(p... ob.

where the first uncertainty is statistical, the second reflects all systematic effects apart from that arising the luminosity, which is given as the third uncertainty. Differential cross-sections are also presented as functions of the Z-boson rapidity and of the angular variable ϕ^*, which is related to the Z-boson transverse momentum.

Measurement of the $Z + b$-jet cross-section in pp collisions at $\sqrt{s} = 7\,\mathrm{TeV}$ in the forward region

JHEP01 (2015) 064 arXiv:1411.1264

Abstract

The associated production of a Z boson or an off-shell photon γ^* with a bottom quark in the forward region is studied using proton-proton collisions at a centre-of-mass energy of 7 TeV. The Z bosons are reconstructed in the $Z/\gamma^* \to \mu^+\mu^-$ final state from muons with a transverse momentum larger than 20 GeV, while two transverse momentum thresholds are considered for jets (10 GeV and 20 GeV). Both muons and jets are reconstructed in the pseudorapidity range $2.0 < \eta < 4.5$. The results are based on data corresponding to $1.0\,\mathrm{fb}^{-1}$ recorded in 2011 with the LHCb detector. The measurement of the Z+b-jet cross-section is normalized to the Z+jet cross-section. The measured cross-sections are

$$\sigma(\mathrm{Z}/\gamma^*(\mu^+\mu^-)\text{+b-jet}) = 295 \pm 60\ (\mathrm{stat}) \pm 51\ (\mathrm{syst}) \pm 10\ (\mathrm{lumi})\,\mathrm{fb}$$

for $p_{\mathrm{T}}(\mathrm{jet}) > 10\,\mathrm{GeV}$, and

$$\sigma(\mathrm{Z}/\gamma^*(\mu^+\mu^-)\text{+b-jet}) = 128 \pm 36\ (\mathrm{stat}) \pm 22\ (\mathrm{syst}) \pm 5\ (\mathrm{lumi})\,\mathrm{fb}$$

for $p_{\mathrm{T}}(\mathrm{jet}) > 20\,\mathrm{GeV}$.

Motivation

arXiv:0808.1847

Electroweak measurements in the forward region

- probe pQCD and electroweak theory in a novel region of (x, Q^2) phase space;
- constrain PDFs at low x and high Q^2.

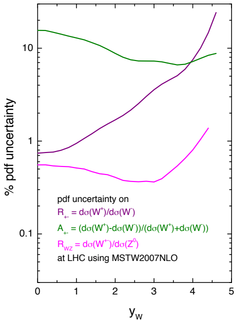

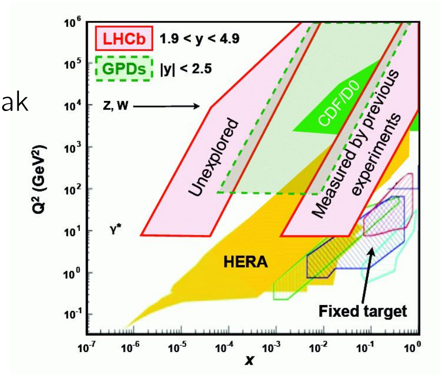

- PDF uncertainties become particularly large at forward boson rapidities;
- LHCb ideally placed to contribute.

Motivation – NNPDF3.0

arXiv:1410.8849

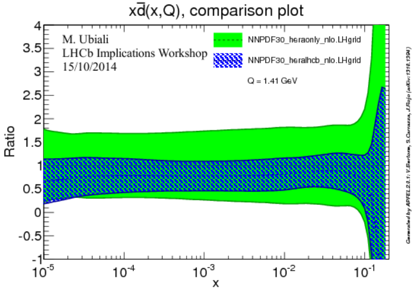

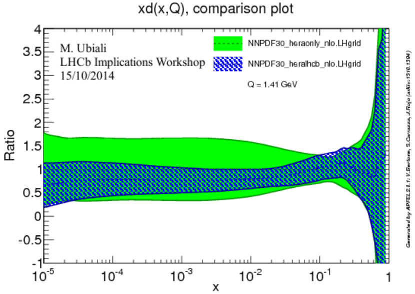

The impact of our early ($37\,\mathrm{pb}^{-1}$) $W \to \mu\nu$ (JHEP06 (2012) 58) and $Z \to ee$ (JHEP02 (2013) 106) measurements is clearly visible.

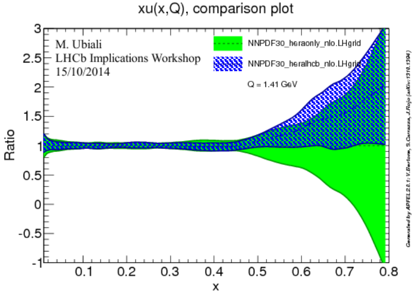

Motivation – ABM12

Phys. Rev. D 89 (2014) 054028

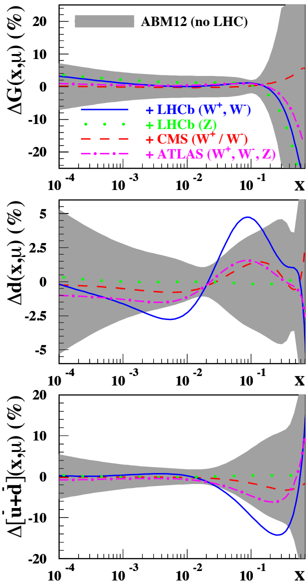

Early LHCb data of W production provide the largest impact on valence d and sea light quark PDFs.

LHCb detector

arXiv:1412.6352 JINST3 (2008) S08005

- Single arm spectrometer optimised for the study of B and D decays;
- Limited to $\sim 4\%$ of the solid angle;
- Corresponds to $2 < \eta < 5$, $\eta \equiv -\ln\left[\tan\left(\frac{\theta}{2}\right)\right] \approx y$;
- Collected $1\,\mathrm{fb}^{-1}$ at $7\,\mathrm{TeV}$ and $2\,\mathrm{fb}^{-1}$ at $8\,\mathrm{TeV}$.

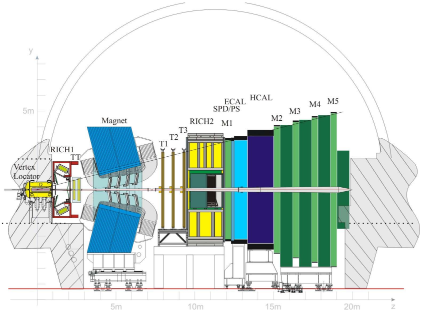

- $\frac{\Delta p}{p} = 0.4\%@5\,\mathrm{GeV}$ and $0.6\%@100\,\mathrm{GeV}$;
- $\sigma(IP) = 20\mu\mathrm{m}$;
- $\epsilon_{track} > 96\%$;
- $\epsilon_{PID}(\mu) \sim 97\%$ with MisID$(\pi \to \mu)$~ $1-3\%$.
- $\epsilon_{PID}(K) \sim 95\%$ with MisID$(\pi \to K)$~ 5%.

Inclusive W – analysis strategy

JHEP12 (2014) 079

- The signal yield is determined from a fit to p_T^μ;
- Signal and electroweak templates are taken from simulation;
- The decay in flight, $K/\pi \to \mu\nu$, component floats freely in the fit with a template determined from data;
- Purities are determined to be $\sim 77\%$.

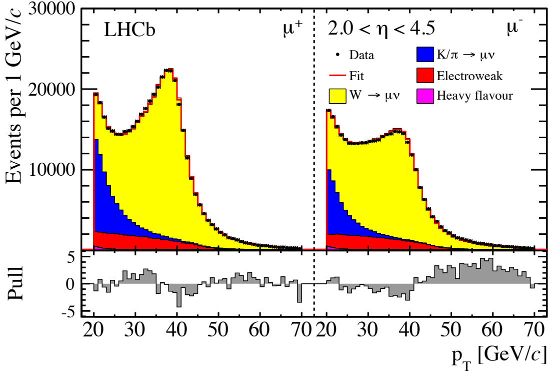

Inclusive W – results

JHEP12 (2014) 079

$\sigma_{W\to\mu\nu}$ cross-section at 7 TeV is measured to be

$$\sigma_{W^+\to\mu^+\nu} = 861.0 \pm 2.0\,(stat.) \pm 11.2\,(syst.) \pm 14.7\,(lumi.)\text{pb}$$

$$\sigma_{W^-\to\mu^-\nu} = 675.8 \pm 1.9\,(stat.) \pm 8.8\,(syst.) \pm 11.6\,(lumi.)\text{pb}$$

The cross-section ratio is measured to be

$$\frac{\sigma_{W^+\to\mu^+\nu}}{\sigma_{W^-\to\mu^-\nu}} = 1.274 \pm 0.005\,(stat.) \pm 0.009\,(syst.)$$

- Results are given at Born-level;
- Theory prediction is from FEWZ at NNLO;
- A selection of NNLO PDF sets are used.

$$p_T^\mu > 20\,\text{GeV}$$
$$2.0 < \eta^\mu < 4.5$$

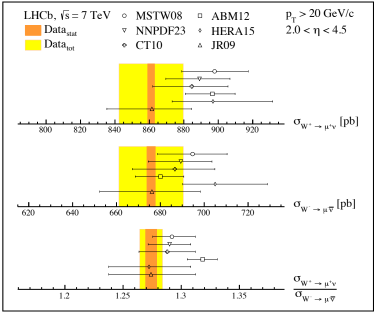

Inclusive W – differential cross-sections

JHEP12 (2014) 079

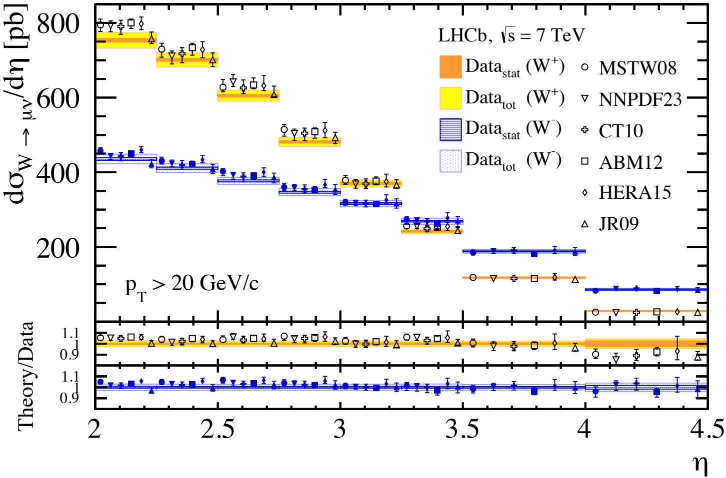

Inclusive W – cross-section ratio and the charge asymmetry

JHEP12 (2014) 079

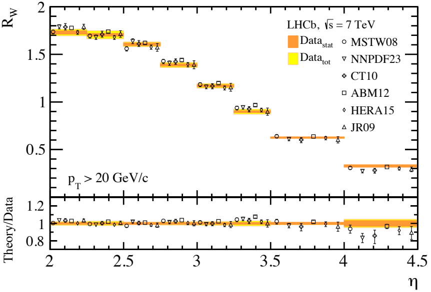

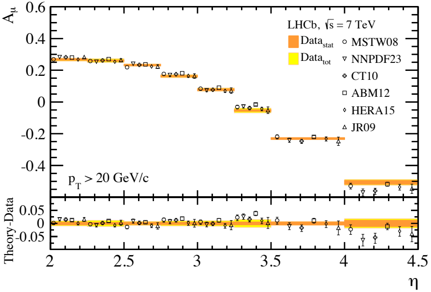

$$R(\eta_\ell) \equiv \frac{\frac{d\sigma^{W^+}}{d\eta_\ell}}{\frac{d\sigma^{W^-}}{d\eta_\ell}}$$

$$\mathcal{A}(\eta_\ell) \equiv \frac{\frac{d\sigma^{W^+}}{d\eta_\ell} - \frac{d\sigma^{W^-}}{d\eta_\ell}}{\frac{d\sigma^{W^+}}{d\eta_\ell} + \frac{d\sigma^{W^-}}{d\eta_\ell}}$$

The measured cross-sections are in agreement with NNLO predictions using different PDF sets.

Inclusive W – comparison to ATLAS

JHEP12 (2014) 079

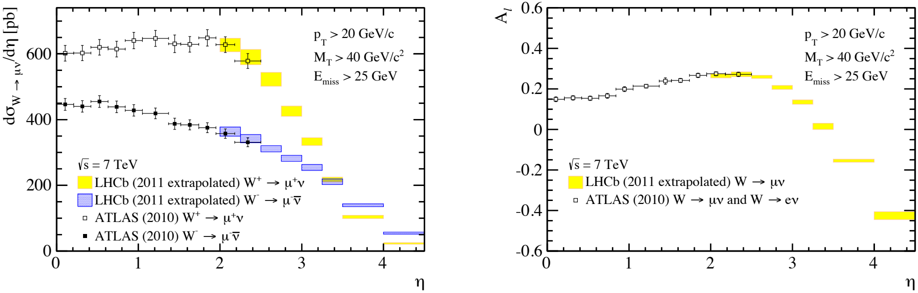

Inclusive W/Z cross-sections at LHCb are complementary to ATLAS (and also to CMS).

Inclusive Z – results

LHCb-PAPER-2015-003

$\sigma_{Z\to e^+e^-}$ cross-section at 8 TeV is measured to be

$$\sigma_{Z\to e^+e^-} = 93.81 \pm 0.41\,(stat.) \pm 1.48\,(syst.) \pm 1.14\,(lumi.)\,\mathrm{pb}$$

- Results are given at Born-level;
- Theory prediction is from FEWZ at NNLO;
- A selection of NNLO PDF sets are used;
- Correlation matrices for bins of y_Z and ϕ^* are provided for PDF fitters.

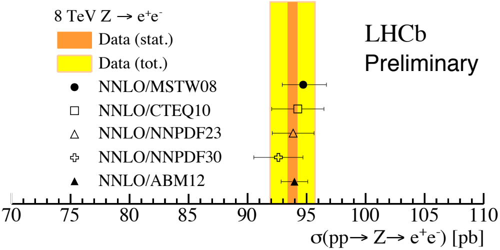

$$p_{\mathrm{T}}^{e} > 20\,\mathrm{GeV}$$
$$2.0 < \eta^{e} < 4.5$$
$$60 < M_{ee} < 120\,\mathrm{GeV}$$

Inclusive Z – differential cross-sections

LHCb-PAPER-2015-003

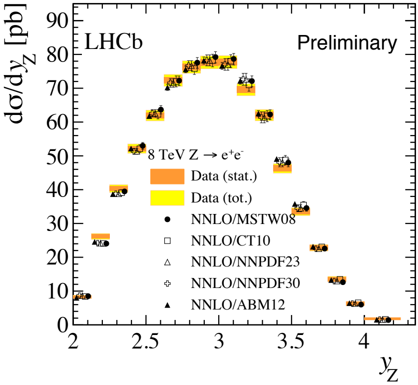

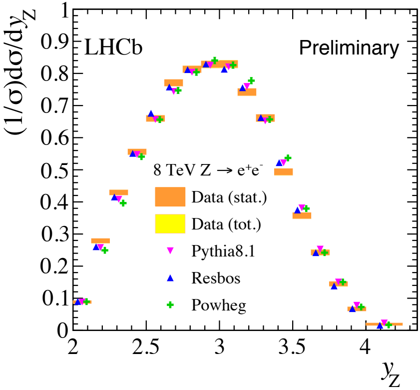

The measured cross-sections are in agreement with NNLO predictions using different PDF sets.

Inclusive Z – differential cross-sections

LHCb-PAPER-2015-003

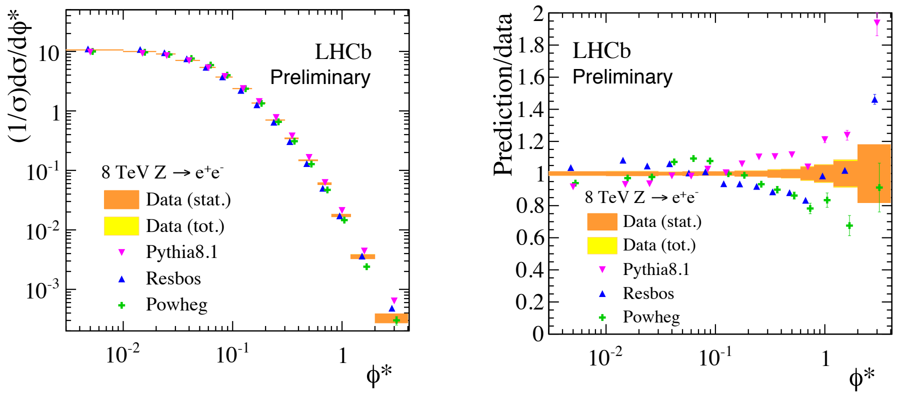

$$\phi^* \equiv \tan(\phi_{acop}/2)/\cosh(\Delta\eta/2) \approx p_{\mathrm{T}}/M,$$

where $\phi_{acop} \equiv \pi - |\Delta\phi|$, $\Delta\eta$ is measured between leptons and M, p_{T} are the invariant mass and transverse momentum of the lepton pair.

$Z + b$-jet – jet reconstruction and ID

JHEP01 (2015) 064

- Builds on the Z+jet result (JHEP01 (2014) 033);
- Jets formed using particle flow with the anti-k_T algorithm;
- b-tagging efficiency taken from simulation (dominant systematic uncertainty).

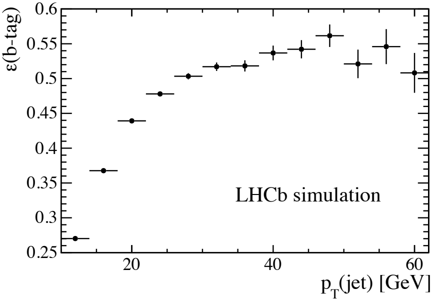

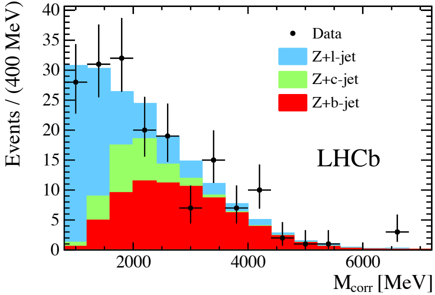

- A selection that forms displaced vertices is used to enrich the sample with b-jets;
- b-jet yield is extracted from a $\mathscr{L}$-fit to the corrected mass;
- Templates for b, c, l-jets are obtained from simulation.

$Z + b$-jet – results

JHEP01 (2015) 064

$\sigma_{Z\to\mu\mu+b-jet}$ cross-section at 7 TeV for $p_{\mathrm{T}}^{jet} > 10\,\mathrm{GeV}$,

$$\sigma(Z+b-jet) = 295 \pm 60\,(stat.) \pm 51\,(syst.) \pm 10\,(lumi.)\mathrm{fb}$$

for $p_{\mathrm{T}}^{jet} > 20\,\mathrm{GeV}$,

$$\sigma(Z+b-jet) = 128 \pm 36\,(stat.) \pm 22\,(syst.) \pm 5\,(lumi.)\mathrm{pb}$$

- Theory prediction from MCFM;
- Theory uncertainties account for PDFs, scales;
- A correction for showering and hadronisation is taken from simulation.

$$p_{\mathrm{T}}^{\mu} > 20\,\mathrm{GeV}$$
$$2.0 < \eta^{\mu,jet} < 4.5$$
$$60 < M_{\mu\mu} < 120\,\mathrm{GeV}$$
$$\Delta r(jet,\mu) > 0.4$$

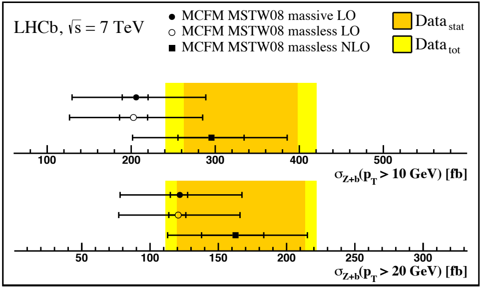

Summary and outlook

- LHCb continues to build on past successes in its electroweak program;
- We are successfully branching into jet physics;
- Our measurements are seen to have an impact on PDFs;
- The higher energies of Run II allow us to probe lower x values.

Appendix

LHCb phase space

While ATLAS&CMS are largely limited to $\eta \leq 2.5$ (with Bjorken-x in the range of $10^{-3} \leq x \leq 0.1$), LHCb detects W and Z daughters in $2 < \eta < 5$. These are formed in a highly boosted system with respect to the lab frame with one parton at $x_a \sim 0.1$ and the other at $x_b \sim 10^{-4}$.

$$y_{W(Z)} = \ln\left(\frac{x_a}{x_b}\right)^{\frac{1}{2}} \Longrightarrow x_{a,b} = \frac{M_{W(Z)}}{\sqrt{s}} e^{\pm y_{W(Z)}}$$

Flavour decomposition of W

Eur. Phys. J. C 14 (2000) 133

- σ_W is sensitive to the flavour composition of the quark sea;
- Can be used in constraining the strange PDF.

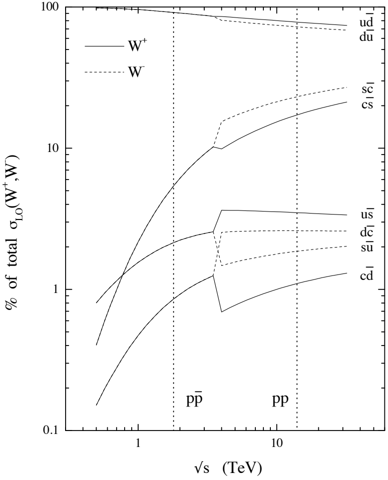

Charge asymmetry

Phys. Rev. D 69 (2004) 094008

The charge asymmetry is given as

$$\mathscr{A}(\eta_\ell) \equiv \frac{\frac{d\sigma^{W^+}}{d\eta_\ell} - \frac{d\sigma^{W^-}}{d\eta_\ell}}{\frac{d\sigma^{W^+}}{d\eta_\ell} + \frac{d\sigma^{W^-}}{d\eta_\ell}} \approx \frac{u-d}{u+d} \approx \frac{u_{val} - d_{val}}{u_{val} + d_{val} + 2u_{sea}}$$

- $\mathscr{A}(\eta_\ell)$ is almost completely insensitive to higher order QCD corrections;
- several experimental uncertainties also cancel;
- a measurement of this quantity is a powerful probe of PDFs.

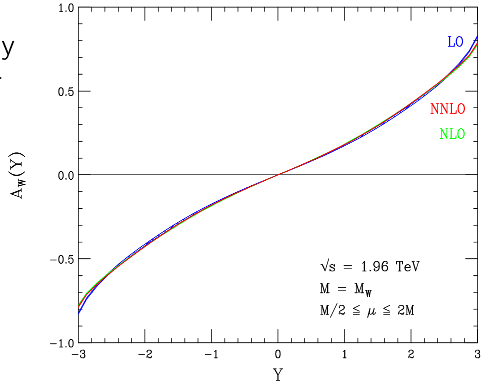

Inclusive W – systematics

JHEP12 (2014) 079

Table 1: Summary of the systematic uncertainties on the inclusive cross-sections and their ratio.

Source	$\Delta\sigma_{W^+\to\mu^+\nu}$ [%]	$\Delta\sigma_{W^-\to\mu^-\overline{\nu}}$ [%]	ΔR_W [%]
Template shape	0.28	0.39	0.59
Template normalisation	0.10	0.10	0.06
Reconstruction efficiency	1.21	1.20	0.12
Selection efficiency	0.33	0.32	0.18
Acceptance and FSR	0.18	0.12	0.21
Luminosity	1.71	1.71	—

Inclusive Z – systematics

LHCb-PAPER-2015-003

Table 1: Efficiencies and other factors used for the cross-section determination, averaged over the experimental acceptance by integrating over y_{Z}. The fractional uncertainties on the overall factors are also given, separated into components that are assumed to be correlated and uncorrelated between bins of y_{Z} or of ϕ^*.

		Fractional uncertainty	
	Average value	Uncorrelated	Correlated
ϵ_{GEC}	0.916		0.006
$\epsilon_{\mathrm{Trig.}}$	0.892	0.001	
$\epsilon_{\mathrm{Track.}}$	0.912	0.001	0.010
$\epsilon_{\mathrm{Kin.}}$	0.507	0.002	0.006
ϵ_{PID}	0.838	0.001	0.007
ϵ	0.319	0.002	0.016
f_{MZ}	0.969	0.001	
Background estimation			0.004
$\int \mathcal{L}\mathrm{d}t$ / pb^{-1}	1976		0.0122

$Z + b$-jet – systematics

JHEP01 (2015) 064

Table 1: Relative systematic uncertainty considered for the Z+b-jet cross-section for p_{T}(jet) > 20 GeV. The relative uncertainties are similar for the 10 GeV threshold. The first four contributions are from Ref. [18].

Source of systematic uncertainty	Relative uncertainty (%)
Z boson reconstruction	3.5
Unfolding	1.5
Jet-energy scale, resolution and reconstruction	7.8
Final-state radiation	0.2
Luminosity	3.5
M_{corr} template and b-tagging	15.0
Jet reconstruction flavour dependence	2.0
Total	17.8

Topological secondary vertex tagger

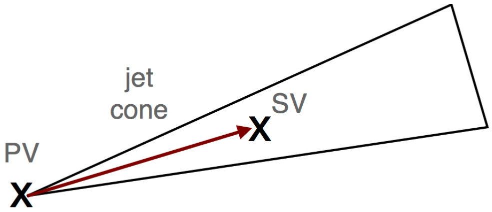

The TOPO tagger forms secondary vertices from combinations of two, three, and four particles within a jet.
If at least 60% of the detector hits that make up the tracks forming the TOPO object also belong to tracks within the jet, then the jet satisfies a b–tag requirement.

Corrected mass

The number of b–jets is extracted from an unbinned likelihood fit to the corrected mass of the TOPO candidate defined as

$$M_{corr} \equiv \sqrt{M^2 + p^2 \sin^2\theta} + p \sin\theta,$$

where M and p are the invariant mass and momentum of all tracks in the jet that are inconsistent with originating directly from a pp collision and have a minimum distance of closest approach to a track used in the TOPO less than $0.2\,\mathrm{mm}$. The angle θ is between the momentum and the direction from the pp collision to the TOPO object vertex.